1D/3D Numerical Approach for Modelling a Milli-Structured Heat Exchanger/Reactor

Antoinette Maarawi[a*], Zoé Anxionnaz-Minvielle[a], Pierre Coste[a], Nathalie Di Miceli Raimondi[b], Michel Cabassud[b]

a Univ. Grenoble Alpes, CEA, LITEN, DTBH, Laboratoire Echangeurs et Réacteurs, F-38000 Grenoble
b Laboratoire de Génie Chimique, Université de Toulouse, CNRS, INPT, UPS, Toulouse, France

antoinette.maarawi@cea.fr

Milli-structured heat exchangers/reactors are one of the intensified technologies, which have been successfully used in the case of exo- or endo-thermal chemical syntheses. Enhanced performances of such technologies compared to conventional apparatuses have been observed. This work is focused on the numerical investigation of the "DeanHex" heat exchanger/reactor with a 2D-meandering square cross-section channel with a hydraulic diameter of 2 mm. Throughout the years, only a part of the corrugated channel had been modelled due to the high ressource consumption of CFD simulations. Therefore, in order to model the reactor in a less resource demanding way than a full 3D approach, a new numerical approach is developed. The $2{\times}2$ mm^2 meandering flow channel, which is the core of the heat exchanger/reactor design, is depicted by a 1D homogeneous model coupled to a 3D model for the surrounding solid in which the channel is embedded. This offers a compromise between the simulation at small scale and the simulation at the reactor scale, giving a great advantage in computational efficiency over meshing and computing 3D channels. In this paper, the 1D/3D approach is validated with heat transfer calculations between the 1D monophasic flow milli-channel and its 3D surrounding using an experimental work previously conducted on the "DeanHex" heat exchanger/reactor.

1. Introduction

Process intensification (PI) has been defined in the literature (Stankiewicz and Moulijn, 2000) as a multidisciplinary engineering approach with the aim of developing innovative technologies, such as compact heat exchangers, that offer more energy-efficient and environmental-friendly processes, with higher productivity and safer operation. Compact heat exchangers with milli- and micro- channels have experienced some developments, like the implementation of corrugated geometries, in the purpose of offering new possibilities of heat transfer enhancement (Kapustenko P.O. et al., 2015). Tan Wei Q. et al. (2018) investigated the effects of corrugated plate geometries on the improvement of the thermo-hydraulic performances of a plate heat exchanger. Moreover, these compact heat exchangers can turn into heat exchangers/reactors when the reacting fluids are introduced at the inlet on one side. The removal or addition of heat for the reaction is thus enhanced because of the intensified heat transfer performances of such technologies. The plate HEX reactor (DeanHex) built by the Laboratoire de Génie Chimique (LGC, France) and the Commissariat à l'Energie Atomique et aux Energies Alternatives (CEA, France) is a fine example of such intensified devices. It consists of a succession of process plates (where the reaction takes place) and utility plates (for cooling or heating), where millimetric channels are engraved by laser machining. In this work, a square process channel of a hydraulic diameter d_h equal to 2 mm with periodic zigzag units is considered. The geometry of the channel is represented in Figure 1. The radius of curvature of the bends R_c, the length of the straight section L_s and the angle between two straight sections θ are equal to 1.5 mm, 7 mm and 90 °, respectively. The interest of this particular corrugated geometry lies in the generation of secondary flow (Dean vortices) which helps improving mixing and heat transfer. In fact, the transition between laminar and turbulent flow in these DeanHex zigzag channels is around a Reynolds

number equal to 200 (Théron et al., 2014). This allows reaching a quasi-plug flow and heat and mass transfer intensification while sufficient residence time is achieved to complete chemical conversion.
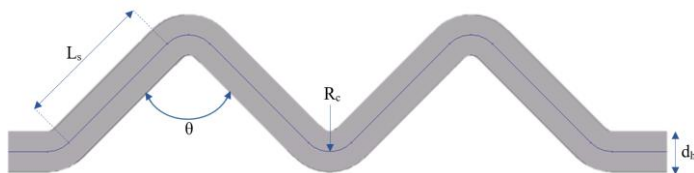

Figure 1: Schematic of the zigzag channel with geometric parameters.

However, from a numerical point of view, the complexity of the geometry, along with the high channel length to hydraulic diameter ratio, make the modelling of such devices with a full 3D approach difficult and very time-consuming regarding the high mesh refinement required in such geometries notably with transitional flow. The full-scale DeanHex reactor has a channel of total developped length of about 6.6 m. In the previous years, only a part of the channel could have been modelled using CFD approaches. Moreau et al. (2017) built a 3D model for the DeanHex channels, using COMSOL Multiphysics 4.3b, allowing the estimation of axial dispersion coefficients from calculated velocity and concentration fields in laminar flow. The simulated channel had a total length of about 0.27 m. Tetrahedral and cubic meshes were used in order to compromise between the simulation accuracy and the computing time. Shi et al. (2019) characterised the flow and heat transfer in the DeanHex square zigzag channel in laminar flow conditions by conducting 3D simulations using the finite volume CFD code, ANSYS CFX 16. Wavy channels with different geometries (L_s=2-12 mm) and a total length of 0.1 m were modelled. The total number of elements needed to mesh the wavy channels of L_s=3.5 mm and L_s=12 mm was about 4.3 million and 7.6 million, respectively. This shows that the 3D modelling of a portion of the wavy channel is highly resource demanding. Therefore, in order to overcome the limitations of CFD simulations of such corrugated channels, this work proposes a new 1D/3D numerical approach that makes the modelling of the whole reactor possible. The full description of this approach is detailed in this paper as well as its validation by a previous experimental work conducted in the DeanHex millimetric zigzag channel.

2. 1D/3D numerical approach description

A full 3D numerical approach allows the direct modelling of local transfer mechanisms in the HEX reactor. However, given the complex geometry of the zigzag channel and the high L/d_h ratio, the 3D simulations are very costly in resources, especially in computing time. Therefore, in order to model the HEX reactor in a less resource demanding way, a new 1D/3D approach has been developed, using COMSOL Multiphysics V5.5. A 1D model is built for the meandering flow channel, using COMSOL's Pipe Flow Module. The latter solves for homogeneous cross sections, which means it performs averaged calculations in the channel's cross-sections. The modelled variables vary only along the length of the channel. Correlations, which were obtained during previous experimental works, are integrated in this 1D model. Consequently, this approach does not only help to avoid meshing the cross section of the channel with a full 3D mesh, but also offers a simulation method that is capable of predicting the performance of the reactor (reaction conversion, selectivity, etc.). The 3D channel is represented by a 1D curve "C" following its axial direction, embedded in a 3D surrounding solid "S". However, as seen from the solid matrix, the boundary condition between the channel and "S" is imposed by the channel on its axis "C" which is a line without any cross-section. In reality, this boundary condition is imposed on the walls of the channel with a 2×2 mm² cross-section, not on the axis. Therefore, in the present work, the cross-section of the millimetric zigzag channel, being non-negligible compared to the whole HEX reactor, must be taken into account in the model in order to correctly represent the DeanHex reactor. Consequently, the proposed solution is to define, around the curve "C", the three-dimensional channel "S2" as shown in Figure 2. Then a thermal chain "C-S2-S" is established to transmit the boundary condition from "C" to the walls of "S2". A sensitivity study was carried out in order to determine the material properties of "S2" (density ρ (kg·m^{-3}), specific heat capacity C_p (J·kg^{-1}·K^{-1}) and thermal conductivity λ (W·m^{-1}·K^{-1})). The variations of the density and heat capacity of "S2" have showed no influence on the simulated thermal profiles. However, the effect of the radial thermal conductivity is clearly observed. As expected, by increasing λ to about 1000 W·m^{-1}·K^{-1}, the propagation of the temperature boundary condition from the channel "C" to the wall of "S2" is improved. Above this value, no more effect is observed on the thermal profiles. Consequently, to stay on the safe side, a radial thermal conductivity of 10^5 W·m^{-1}·K^{-1} is applied to "S2" to transmit the "thermal information" from "C" to the walls of "S2", regardless of the system conditions.
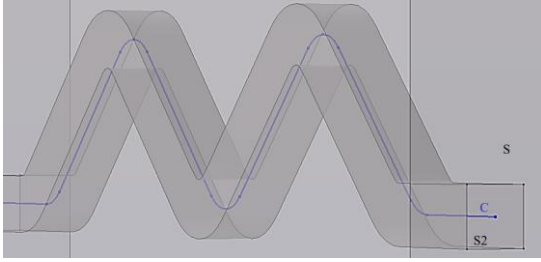
Figure 2: Illustration of the simulated geometry using the 1D/3D approach.

Since the geometry of the studied millimetric channel is composed of periodic zigzag units, imposing a radial infinite conductivity to "S2" requires the definition of a new curvilinear coordinate system (cc) for "S2". It allows the generation of a new base of vectors (ccx, ccy, ccz) at any point of "S2", as shown in Figure 3. The thermal conductivity of "S2" is thus defined according to this curvilinear coordinate system: infinite (equal to 10^5 W·m^{-1}·K^{-1}) along ccy and ccz (green and blue vectors respectively) and zero along ccx (red vector).
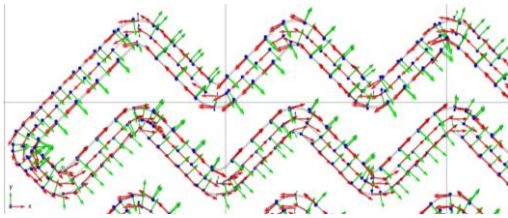

Figure 3: The new curvilinear coordinate system applied to the 3D zigzag channel.

3. Model equations

For incompressible fluid at steady state, the 1D pipe flow module calculates the pressure, velocity and temperature by solving the following momentum (Eq(1)), continuity (Eq(2)) and energy balance (Eq(3)) equations inside the channel referred to as the "process channel " (subscript p):

$$\rho_p u_p \cdot \nabla u_p = -\nabla p_p - f_D \frac{\rho_p}{2d_{h,p}} u_p |u_p| \tag{1}$$

$$\nabla \cdot (A_p \rho_p u_p) = 0 \tag{2}$$

$$\rho_p A_p C_{p,p} u_p \cdot \nabla T_p = \nabla \cdot A_p \lambda_p \nabla T_p + f_D \frac{\rho_p A_p}{2d_{h,p}} |u_p|^3 + Q_{wall} \tag{3}$$

$$Q_{wall} = h_p Z_p (T_S - T_p) \tag{4}$$

u_p is the cross-section averaged velocity (m·s^{-1}), p_p the pressure (Pa), T_p the process fluid temperature (K), f_D the Darcy friction factor (dimensionless). The process fluid (water) physico-chemical properties such as ρ_p the density (kg·m^{-3}), $C_{p,p}$ the heat capacity at constant pressure (J·kg^{-1}·K^{-1}) and λ_p the thermal conductivity (W·m^{-1}·K^{-1}) are assumed variable in function of T_p. A_p is the theoretical pipe cross-sectional area (m^2) and $d_{h,p}$ the mean hydraulic diameter (m) of the process channel. f_D is correlated to Reynolds number Re_p for the millimetric zigzag channel as shown in Eq(5) (Théron et al., 2014). The Reynlods number in the channel is calcuated using Eq(6), where μ is the fluid viscosity (Pa·s).

$$f_D = 24.3 Re_p^{-0.71} \; for \; 20 < Re_p < 200$$
$$f_D = 6 Re_p^{-0.43} \; for \; Re_p > 200 \tag{5}$$

$$Re = \frac{\rho \cdot u \cdot d_h}{\mu} \tag{6}$$

Furthermore, Q_{wall} is the heat exchanged (W·m⁻¹) across the channel's wall (Eq(4)), h_p the convective heat transfer coefficient inside the channel (W·m⁻²·K⁻¹), Z_p the wetted perimeter of the channel (m) and T_S the temperature (K) of the 3D surrounding solid. In this work, h_p is calculated from a Nusselt number correlation Nu_p (dimensionless) established for the DeanHex millimetric zigzag channel (Anxionnaz et al., 2011):

$$\text{Nu}_p = \frac{h_p d_{h,p}}{\lambda_p} = 0.16 Re_p^{0.66} Pr_p^{0.33} \tag{7}$$

Where Re_p and Pr_p are the Reynolds and Prandtl dimensionless numbers in the process channel, respectively. The Prandtl number is calculated as follows:

$$Pr = \frac{C_p \cdot \mu}{\lambda} \tag{8}$$

In addition, the resolved heat balance equation for the 3D surrounding solid "S" is given by:

$$\nabla \cdot (-\lambda_S \nabla T_S) = \nabla \cdot q_u \tag{9}$$

Where λ_s is the thermal conductivity (W·m⁻¹·K⁻¹) of "S" and q_u the heat flux boundary condition (W·m⁻²) imposed on the walls of "S". The latter wil be further described in the following, where the subscript u refers to the "utility channel ".

4. Experiments vs 1D/3D simulations

4.1 Description

The validation of the proposed 1D/3D approach is discussed by comparing the simulated results to experimental ones. The experimental work of Théron et al. (2014), in which thermo-hydraulic performances of the DeanHex millimetric zigzag channel had been characterised, is used. During this study, the HEX reactor consisted of a succession of three process plates sandwiched between four utility plates. 2 mm square cross-section channels, with periodic zigzag units, were engraved on both plates by laser machining. The process and utility streams are separated by a 2 mm metal thickness (closing plates). In the present work, only the first process plate is modelled (Figure 4a). The computational domains consist of a three-dimensional zigzag channel of total length equal to 2.2 m "S2" with a radially infinite thermal conductivity, centered by a one-dimensional zigzag curve "C". "S2" is surrounded, from both sides, by a metallic solid matrix "S" of 2 mm thickness, representing the closing plates. The thermal chain "C-S2-S" is thus established as shown closely in Figure 4b. Nonetheless, the utility channels do not take part in the computational domains but are replaced by heat flux boundary conditions q_u at the upper and lower walls of "S":

$$q_u = h_u(T_S - T_u) \tag{10}$$

Where T_u is the utility fluid temperature (K). The convective heat transfer coefficient h_u (W·m⁻²·K⁻¹) in the zigzag utility channels is deduced from the Nusselt correlation (Eq(11)) proposed by Shi (2019):

$$Nu_u = \frac{h_u d_{h,u}}{\lambda_u} = 0.2(Re_u^{0.67} + 8.9) Pr_u^{0.3} \left(\frac{d_{h,u}}{L_{s,u}}\right)^{0.4} \tag{11}$$

Where Re_u and Pr_u are the Reynolds and Prandtl dimensionless numbers for the utility side, repectively. $d_{h,u}$ and $L_{s,u}$ are, correspondingly, the hydraulic diameter (m) and the straight length (m) between the bends in the utility zigzag channel. λ_u is the thermal conductivity of the utility fluid (water) estimated at T_u as for all the other physicochemical properties of the utility fluid. A correction factor $\frac{A_u}{A_S}$ is applied to q_u to consider the difference of heat transfer areas between the utility channels (A_u, m²) and the walls of "S" (A_s, m²). A_u is the heat transfer area of the utility channels which can be calculated using Eq(12):

$$A_u = P_u . L_u . N_u \tag{12}$$

Where P_u and L_u are correspondingly the perimeter (m) and the total developed length (m) of the utility channel. N_u is the number of utility channels engraved on one utility plate. Note that, the utility plate that is below the first process plate of the pilot, exchanges heat with the first and second process plates. Therefore, $\frac{1}{2}P_u$ is used when imposing the heat flux boundary condition on the bottom side of "S". A free tetrahedral meshing is applied to the 3D domains where only thermal conduction occurs. Consequently, there is no need for a refined finely constructed meshing. Furthermore, the experimental conditions in Théron et al. (2014) are applied to the model and are presented in Table 1.

Table 1: Operating conditions applied for the simulations

Utility Side		Process Side	
Q_u (kg·h^{-1})	T_u (°C)	Q_p (kg·h^{-1})	T_p (°C)
≈152	≈15.6	2.4 4 5.5 6.9	≈76

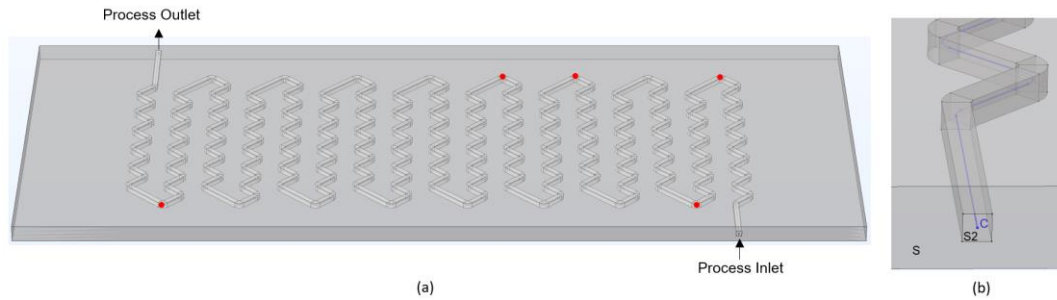(a)   (b)

Figure 4: Illustrations from the 1D/3D model of: (a) the process plate with the inlet and outlet of the flow (in red: the position of thermocouples in the experiments) and (b) a zoom-in on the process inlet where the C-S2-S chain is showed.

4.2 Results

Since for the experiments the heat transfer process is not limited by the utility side, the comparison of the 1D/3D simulation results with experimental results will reveal any error that could be made on the process side and thus the proposed approach will be appropriately evaluated. In Figure 5, the temperature evolution is represented in function of the axial position of the process channel, for different "process" flowrates. In the experiments, 5 K-type thermocouples were located along the first process channel, thus a part of the thermal profile is observed (Théron et al., 2014). As shown in Figure 5, the simulated process thermal profiles are in good agreement with the experimental measurements. One aberrant point is observed and corresponds to the temperature measured at 0.28 m from the inlet. This discrepancy, observed for all the curves, can be explained by a misplacement of the thermocouple during the experiments. All the simulated temperatures at this point are higher than that measured by this thermocouple. In fact, the fluid flowing through the process channel is normally hotter than the plate material. Therefore, the probe maybe in contact with the material of the plate instead of being inserted in the flowing fluid. Regardless this point, the maximum relative error is less than 8 %, which is assumed acceptable. Consequently, the 1D/3D approach with the radially infinite thermal conductivity imposed for "S2" is validated considering these experimental data.
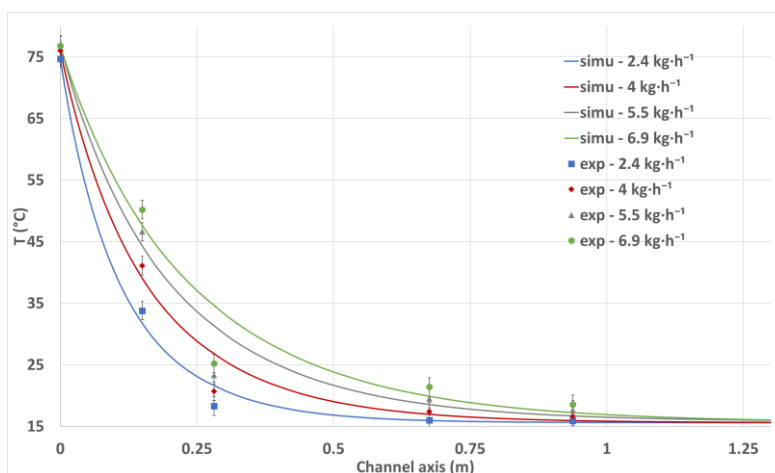

Figure 5: Evolution of experimental and simulated process fluid temperature along the process channel for different process flowrates.

5. Conclusions

A new 1D/3D numerical approach is proposed in this work in order to model the DeanHex zigzag channel in a less resource demanding way than CFD approaches. The latters allow the simulation of only few zigzag periodic units with a high CPU cost. However, avoiding the 3D meshing of the channel, by using the proposed 1D/3D approach, reduces significantly the computational time to about few minutes and allows the modelling of the full-scale heat exchanger/reactor at a reasonable CPU cost. By comparing the 1D/3D simulated temperature results with experimental ones for one process plate of a 2.2 m long zigzag channel, a maximum relative error less than 8 % is observed. Thus, the 1D/3D approach seems promising and shows a great potential for the purpose of predicting the performance of the whole reactor. This leads to the the next step which consists of completing the heat transfer model by a mass transfer model and to validate it with experimental results. The present work is a first step towards addressing the scale-up issue of "DeanHex" reactors. Expecting a future industrialisation of such equipment, a generalised scaled-up model will be used to predict the performance of the reactor in terms of conversion rate and energy efficiency at industrial scale.

References

Anxionnaz, Z., Theron, F., Tochon, P., Couturier, R., Bucci, P., Vidotto, F., Gourdon, C., Cabassud, M., Lomel, S., Bergin, G., Bouti, S., Peerhossaini, H., Lemenand, T., Habchi, C., 2011. RAPIC project: Toward competitive heat-exchanger/reactors. The 3rd European Process Intensification Conference (EPIC).

Kapustenko P.O., Kukulka D.J., Arsenyeva O.P., 2015. Intensification of heat transfer processes. Chemical Engineering Transactions 45, 1729–1734. https://doi.org/10.3303/CET1545289

Moreau, M., Di Miceli Raimondi, N., Le Sauze, N., Gourdon, C., Cabassud, M., 2017. A new numerical method for axial dispersion characterization in microreactors. Chemical Engineering Science 168, 178–188. https://doi.org/10.1016/j.ces.2017.04.040

Shi, H., 2019. Etude du transfert de chaleur en canaux millimétriques de type zigzag pour le développement et l'extrapolation de réacteurs-échangeurs compacts. Université Toulouse 3 - Paul Sabatier.

Shi, H., Di Miceli Raimondi, N., Fletcher, D.F., Cabassud, M., Gourdon, C., 2019. Numerical study of heat transfer in square millimetric zigzag channels in the laminar flow regime. Chemical Engineering and Processing - Process Intensification 144, 107624. https://doi.org/10.1016/j.cep.2019.107624

Stankiewicz, A., Moulijn, J., 2000. Process Intensification: Transforming Chemical Engineering. Chemical Engineering Progress 22–34.

Tan Wei Q., Sun Li, Jia Zhigang, Li Jie, 2018. Thermal-hydraulic performance analysis of corrugated plate heat exchanger. Chemical Engineering Transactions 70, 1153–1158. https://doi.org/10.3303/CET1870193

Théron, F., Anxionnaz-Minvielle, Z., Cabassud, M., Gourdon, C., Tochon, P., 2014. Characterization of the performances of an innovative heat-exchanger/reactor. Chemical Engineering and Processing: Process Intensification 82, 30–41. https://doi.org/10.1016/j.cep.2014.04.005